

Accepted Manuscript

Synthesis, biological evaluation, and molecular docking investigation of 3-amidoindoles as potent tubulin polymerization inhibitors

Peng Chen, Yu-Xin Zhuang, Peng-Cheng Diao, Fang Yang, Shao-Yu Wu, Lin Lv, Wen-Wei You, Pei-Liang Zhao



PII: S0223-5234(18)30997-8

DOI: <https://doi.org/10.1016/j.ejmech.2018.11.038>

Reference: EJMECH 10895

To appear in: *European Journal of Medicinal Chemistry*

Received Date: 15 July 2018

Revised Date: 29 October 2018

Accepted Date: 16 November 2018

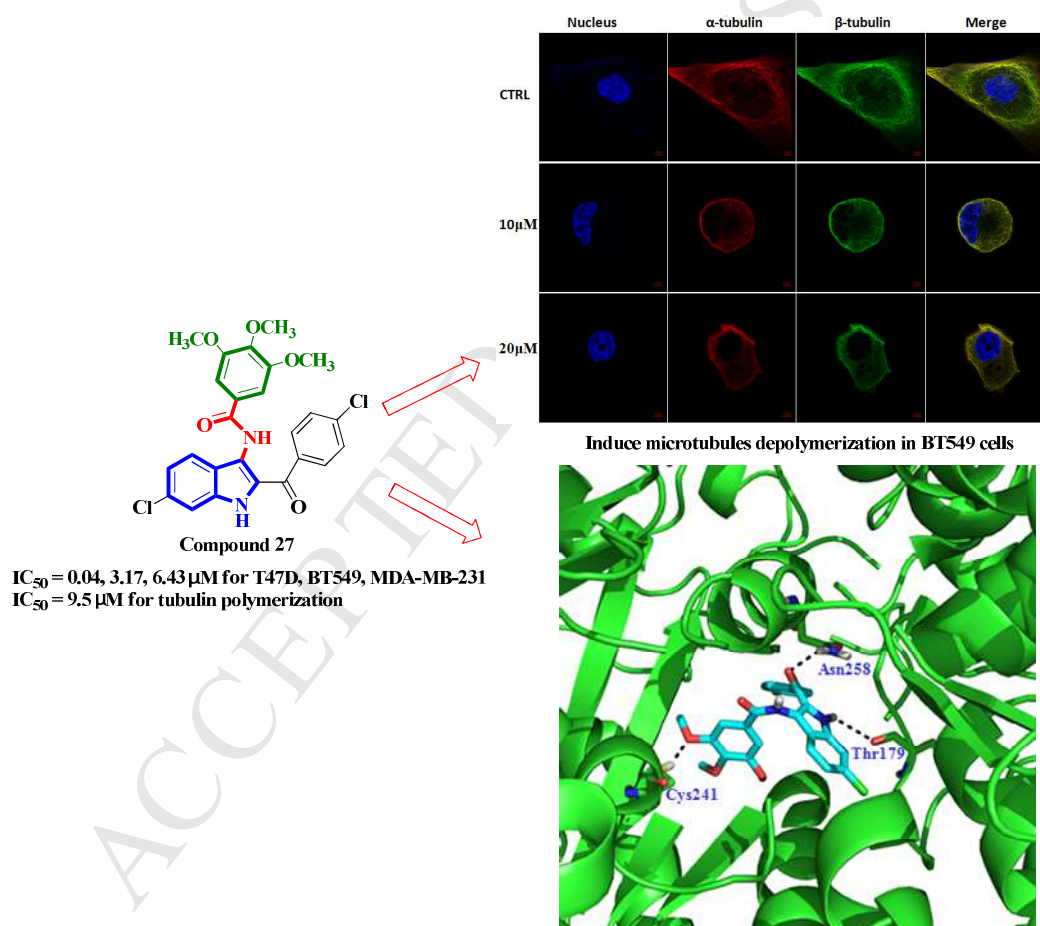
Please cite this article as: P. Chen, Y.-X. Zhuang, P.-C. Diao, F. Yang, S.-Y. Wu, L. Lv, W.-W. You, P.-L. Zhao, Synthesis, biological evaluation, and molecular docking investigation of 3-amidoindoles as potent tubulin polymerization inhibitors, *European Journal of Medicinal Chemistry* (2018), doi: <https://doi.org/10.1016/j.ejmech.2018.11.038>.

This is a PDF file of an unedited manuscript that has been accepted for publication. As a service to our customers we are providing this early version of the manuscript. The manuscript will undergo copyediting, typesetting, and review of the resulting proof before it is published in its final form. Please note that during the production process errors may be discovered which could affect the content, and all legal disclaimers that apply to the journal pertain.

Synthesis, biological evaluation, and molecular docking investigation of 3-amidoindoles as potent tubulin polymerization inhibitors

Peng Chen[#], Yu-Xin Zhuang[#], Peng-Cheng Diao, Fang Yang, Shao-Yu Wu, Lin Lv^{*}, Wen-Wei You^{*}
Pei-Liang Zhao^{*}

Guangdong Provincial Key Laboratory of New Drug Screening, School of Pharmaceutical Science, Southern Medical University, Guangzhou 510515, P.R.China



Synthesis, biological evaluation, and molecular docking investigation of 3-amidoindoles as potent tubulin polymerization inhibitors

Peng Chen[#], Yu-Xin Zhuang[#], Peng-Cheng Diao[#], Fang Yang, Shao-Yu Wu, Lin Lv^{*}, Wen-Wei
5 You^{*}, Pei-Liang Zhao^{*}

*Guangdong Provincial Key Laboratory of New Drug Screening, School of Pharmaceutical
Science, Southern Medical University, Guangzhou 510515, P.R.China*

10 **ABSTRACT:** A series of novel 3-amidoindole derivatives possessing 3,4,5-trimethoxyphenyl
groups were synthesized and evaluated for their antiproliferative and tubulin polymerization
inhibitory activities. Some of them demonstrated moderate to potent activities *in vitro* against six
cancer cell lines including MCF-7, MDA-MB-231, BT549, T47D, MDA-MB-468, and HS578T.
The most active compound **27** inhibited the growth of T47D, BT549, and MDA-MB-231 cell lines
15 with IC₅₀ values at 0.04, 3.17, and 6.43 μM, respectively. Moreover, the flow cytometric analysis
clearly revealed that compound **27** significantly inhibited growth of breast cancer cells through
arresting cell cycle in G2/M phase *via* a concentration-dependent manner. In addition, the
compound also exhibited the most potent anti-tubulin activity with IC₅₀ values of 9.5 μM, which
was remarkable, compared to CA-4. Furthermor, molecular docking analysis demonstrated the
20 interaction of the compound **27** at the colchicine-binding site of tubulin. These preliminary results
suggest that compound **27** is a very promising tubulin-binding agent and is worthy of further
investigation aiming to the development of new potential anticancer agents.

25 **Keywords:** Microtubules; 3-Amidoindoles; Antiproliferative activity; Tubulin polymerization

30 ^{*} Corresponding author. E-mail: plzhao@smu.edu.cn (P.-L. Zhao), youww@smu.edu.cn (W.-W. You), lynnlv@smu.edu.cn (L. Lv)

[#] These authors contributed equally to this work.

1. Introduction

Microtubules are the basic components of cell structure and have been an important therapeutic target in tumour cells due to their crucial roles in cell proliferation, trafficking, signaling and migration in eukaryotic cells [1-3]. Microtubule-targeting agents that are able to modulate the microtubule assembly by inhibiting tubulin polymerization or blocking microtubule disassembly have attracted considerable interest in anti-cancer therapy [4-7].

In the last decade, a large number of structurally diverse tubulin polymerization inhibitors have been identified [8-12]. Among them, combretastatin A-4 (CA-4, Figure 1) is one of the most well-known antitubulin agents and its corresponding prodrug salt CA-4P has shown promising results in human cancer clinical trials [13]. Most interestingly, the replacement of *cis*-olefin moiety of CA-4 with indole core led to discover a 3-arylindole (**2**) with potent antitubulin activity. Subsequently, by introducing methylene, sulfur and carbonyl bridges, 3-benzylindole (**3**), 3-arylthioindole (**4**) and 3-aryloxyindole (**5**) have been developed as significant inhibitors of tubulin polymerization with potent antiproliferative activities [14-17]. However, chemical modification of incorporating amido bridge into 3-arylindole was not exhaustively explored. Inspired by these observations and as a part of our continuing effort on the development of nitrogen-containing heterocycles as novel antitumor agents [18-22], we designed a series of novel 3-amidoindole derivatives **6–34** by incorporating an amido bridge into 3-position of indole core (Fig. 1), which have, to our knowledge, not been reported so far. In the present study, we described the detailed synthetic routes, antiproliferative and tubulin polymerization inhibitory activities of these compounds.

<Insert figure 1 here>

2. Chemistry

The synthetic route for target compounds **6–34** was illustrated in Scheme 1. Substituted 2-aminobenzonitriles **35** were converted to the corresponding *N*-ethoxycarbonylanilines **36** by treatment with neat ethyl chloroformate (ClCO₂Et) at reflux. The subsequent condensation, followed by Thorpe–Ziegler cyclization with various α -bromoketones using

potassium carbonate as base in dimethylformamide (DMF) provided the common intermediates *N*-1-ethoxycarbonyl-2-substituted-3-aminoindoles **37**. These intermediates were subsequently converted into the corresponding *N*-unsubstituted indole **38** after alkaline hydrolysis using sodium hydroxide (NaOH) in aqueous ethanol, which had been illustrated in detail in our previously reported approach [23]. Subsequently, the direct nucleophilic substitution of commercially available 3,4,5-trimethoxybenzoyl chloride and 3-amino-1H-indoles **38** in the presence of triethylamine in anhydrous tetrahydrofuran solution gave the desired 3-amidoindole derivatives **6–34** in yields of 54.5–92.1%, respectively. The structures of target compounds **6–34** were characterized with spectroscopic techniques including ¹H NMR, ¹³C NMR, and HRMS spectroscopic techniques, and the spectral data agree with the proposed structures.

<Insert scheme 1 here>

3. Results and Discussion

3.1 *In vitro* antiproliferative activity

All the synthesized 3-amidoindole derivatives **6–34** were evaluated for their *in vitro* antiproliferative activities against a panel of six human cancer cell lines (MCF-7, MDA-MB-231, BT549, T47D, MDA-MB-468, and HS578T) by using MTT assay. The assay results expressed as IC₅₀ (μM) were summarized in Table 1 and compared with the inhibitory activities of a reference compound, CA-4, one of the most potent natural tubulin-binding anticancer agents. Here, the IC₅₀ value represents the concentration of one compound resulting in a 50% inhibition in cell growth after 72 h incubation, and is the average of three independent experiments.

<Insert table 1 here>

Table 1 summarizes the growth inhibitory effects of 3-amidoindole derivatives **6–34** against six human cancer cell lines, with CA-4 as a reference compound. In most cases, the antiproliferative activities of the compounds were greater against the T47D, BT549, and MDA-MB-231 cells compared with the other three cell lines. Among the target 3-amidoindoles, 5 compounds demonstrated potent antiproliferative activities against T47D cell lines with the IC₅₀ value of < 7

μM . While the most active compound identified in this study was derivative **27**, which inhibited the growth of T47D, BT549, and MDA-MB-231 cancer cell lines with IC_{50} values at 0.04, 3.17, and 6.43 μM , respectively.

95 Further analysis clearly revealed that different antiproliferative activities were observed when various substituents R^1 , R^2 groups were introduced into the indole ring. Concerning R^1 substituents at the C-6 position of the indole ring, it is clear that compounds bearing methoxy groups (**32–34**), exhibit generally lower potency than the corresponding derivatives substituted with methyl, chloro, and hydrogen moieties. For the substituent R^2 , compounds with a bulky 4-phenylphenyl or
100 naphthalenyl group (**10**, **17**, **12**) resulted in a drastic reduction in antiproliferative activities against tested cancer cell lines. Furthermore, replacement of the phenyl ring (R^2) with a heterocyclic ring such as a thiazole or a furan moiety led to an almost complete loss in the activity (**11**, **19**, **28**), which indicated that the phenyl substitution on the indole ring might played a crucial role in modulating the antitumor activity. In addition, a comparison of substituent effects revealed that replacement of
105 the electron-donating groups on the phenyl ring with electron-withdrawing atoms strongly increased growth inhibitory properties (**6**, **9** versus **7**, **8** and **16** versus **14**, **15**, **18**, **20** and **26**, **27** versus **22**, **23**, **25**).

To investigate the mechanism of action of these compounds on cancer cells, one represented analogue **27** was evaluated for the influence on the cell cycle progression. In this study, BT549 cells
110 were treated with 2, 4 and 8 μM concentrations of compound **27** for 24 h. As shown in Fig. **2**, analogue **27** displayed 26.29% (2 μM), 35.92% (4 μM), and 56.58% (8 μM) of cell accumulation in G₂/M phase respectively, whereas in control (untreated cells) 8.88% and CA-4 (positive control, 8 μM) 72.90% of G₂/M phase were observed. These data clearly suggested that compound **27** induced a significant cell cycle arrest at the G₂/M phase in a concentration-dependent manner,
115 compared to untreated cells.

<Insert figure 2 here>

3.2. Immunocytochemistry

120 To confirm the mechanism of action of these compounds, we further investigated the effect of the most active compound **27** on tubulin organization in intact cells, and the microtubule structure

of cells was visualized *via* immunocytochemistry. Confocal images depicted in Fig. 3, displayed that both α -tubulin and β -tubulin microtubules formed an intact network with fine filaments in the untreated BT549 cells. However, cells treated with 10 μ M of **27** for 6 h resulted in significant disruption of both tubulin subtypes, loss of cellular structure, and formation of cell membrane rounding. Furthermore, a 6 h exposure of BT549 cells to 20 μ M of compound **27** led to an absolute loss of microtubule formation (microtubules became short and wrapped around the nucleus) and remarkably affected the cell shape (turned round). These results reveal that compound **27** acts as an antitubulin inhibitor by blocking cell cycle progression and metaphase by disrupting spindle assembly.

<Insert figure 3 here>

3.3. Inhibition of *in vitro* tubulin polymerization

To investigate whether the antiproliferative activities of these derivatives were related to an interaction with the microtubule system, eleven representative active compounds were selected for the evaluation of their *in vitro* inhibitory activities against tubulin polymerization at 10 μ M concentration, and CA-4 was also used as the reference. The results were summarized in Table 2. It was clear that there was a positive correlation between the inhibition of tubulin polymerization and antiproliferative activity of the tested compounds. The most potent compound **27** displayed anti-tubulin activity with an IC_{50} value of 9.5 μ M, which was in the same range as the reference compound CA-4 ($IC_{50} = 4.2 \mu$ M).

<Insert table 2 here>

3.4. Molecular studies

To investigate the possible binding mode for this series of compounds, we selected the most active compound **27** to perform the molecular docking simulations on the colchicine binding site of tubulin. As shown in Fig. 4, the results obtained are similar to those reported for arylindole derivatives, with the trimethoxyphenyl ring in proximity of β Cys241 and the 2-chlorophenyl ring at C-2 position of the indole setting up hydrophobic interactions with the β Lys254, α Val181, β Asn258 and β Met259 side chains [15]. On the other hand, three hydrogen bonds was observed: (i) The

1-NH of the indole ring established a H-bond with α Thr179 (2.2 Å); (ii) The carbonyl group of the 4-chlorobenzoyl moiety forms a hydrogen bond with β Asn258 (2.7 Å). (iii) One of the oxygens of trimethoxyphenyl ring established a H-bond with β Cys241 (2.8 Å).

155

<Insert figure 4 here>

4. Conclusion

In the present study, 3,4,5-trimethoxyphenyl groups were introduced in 3-position of indole cores to generate a series of novel 3-amidoindole derivatives. The antiproliferative activities of the synthesized compounds *in vitro* were evaluated against MCF-7, MDA-MB-231, BT549, T47D, MDA-MB-468, and HS578T cell lines. Most compounds demonstrated significant antiproliferative activity against six human cancer cell lines employed in this study. The IC₅₀ values of the most promising compound **27** were 0.04, 3.17, and 6.43 μ M against T47D, BT549, and MDA-MB-231 cell lines, respectively. Moreover, an immunofluorescence study of compound **27** revealed that its target was most likely tubulin. In addition, the compound **27** also exhibited the most potent anti-tubulin activity with IC₅₀ values of 9.5 μ M, which was remarkable, compared to CA4. These preliminary results demonstrate that compound **27** is a very promising tubulin-binding agent and is worthy of further investigation aiming to the development of new potential anticancer agents.

165

170

5. Experimental protocols

5.1 Chemistry

¹H NMR and ¹³C NMR spectra were recorded on a Mercury-Plus 400 spectrometer in CDCl₃ or DMSO-d₆ solution and chemical shifts were recorded in parts per million (ppm) with TMS as the internal reference. High-resolution mass spectra (HRMS) performed on an Agilent QTOF 6540 mass spectrometer. Melting points (mp) were taken on a Buchi B-545 melting point apparatus and are uncorrected. Unless otherwise noted, reagents were purchased from commercial suppliers and used without further purification while all solvents were redistilled before use.

175

General procedure for the preparation of 3-amidoindole derivatives 6–34.

180

To a solution of 3-amidoindole derivatives **6–34** (1.50 mmol) in THF (10 mL), triethylamine

(0.227 g, 2.25 mmol) was added at 0°C. At this temperature, the reaction mixture was stirred for 20 min before the addition of 3,4,5-trimethoxybenzoyl chloride (2.25 mmol) in dry THF (5 mL). The resulting mixture was stirred at room temperature for 6 h and was then concentrated on a rotary evaporator. The crude product obtained was poured into 20 mL of water and extracted with dichloromethane. The combined organic extracts was dried over anhydrous MgSO₄ and concentrated in vacuo. The crude residue was purified by column chromatography using a mixture of petroleum ether and acetone as an eluent to give the white solid compounds in yields of 54.5–92.1%.

5.1.1 *N*-(2-(4-fluorobenzoyl)-6-methyl-1*H*-indol-3-yl)-3,4,5-trimethoxybenzamide (**6**). Yield, 78.0%; mp: 251.2–251.8°C; ¹H NMR (400 MHz, DMSO-*d*₆) δ: 2.44 (s, 3H, CH₃), 3.71 (s, 3H, CH₃O), 3.79 (s, 6H, 2×CH₃O), 6.92–6.97 (m, 3H, ArH), 7.25 (dd, *J*₁ = 8.8 Hz, *J*₂ = 5.2 Hz, 3H, ArH), 7.55 (d, *J* = 8.0 Hz, 1H, ArH), 7.81 (dd, *J*₁ = 4.0 Hz, *J*₂ = 6.0 Hz, 2H, ArH), 10.01 (s, 1H, NH), 11.68 (s, 1H, NH). ¹³C NMR (100 MHz, DMSO-*d*₆) δ: 186.63, 165.43, 152.82, 140.45, 136.85, 135.90, 131.99, 129.78, 122.55, 121.88, 121.66, 119.80, 115.60, 115.39, 112.49, 105.24, 60.48, 56.32, 22.07. HRMS (ESI) *m/z*: calcd for C₂₆H₂₃FN₂O₅ (M+H⁺) 463.1591 found 463.1752.

5.1.2 3,4,5-trimethoxy-*N*-(6-methyl-2-(4-methylbenzoyl)-1*H*-indol-3-yl)benzamide (**7**). Yield, 92.1%; mp: 252.2–252.6°C; ¹H NMR (400 MHz, DMSO-*d*₆) δ: 2.26 (s, 3H, CH₃), 2.44 (s, 3H, CH₃), 3.71 (s, 3H, CH₃O), 3.79 (s, 6H, 2×CH₃O), 6.93 (d, *J* = 4.0 Hz, 2H, ArH), 7.22 (d, *J* = 7.6 Hz, 2H, ArH), 7.27 (s, 1H, ArH), 7.42 (s, 1H, ArH), 7.55 (d, *J* = 8.8 Hz, 1H, ArH), 7.67 (d, *J* = 8.0 Hz, 2H, ArH), 9.99 (s, 1H, NH), 11.61 (s, 1H, NH). ¹³C NMR (100 MHz, DMSO-*d*₆) δ: 187.69, 165.41, 152.78, 142.47, 140.37, 136.73, 136.12, 135.65, 129.90, 129.47, 122.43, 121.89, 119.76, 112.47, 108.15, 105.31, 60.48, 56.32, 22.07. HRMS (ESI) *m/z*: calcd for C₂₇H₂₆N₂O₅ (M+H⁺) 459.1842 found 459.2006.

5.1.3 *N*-(2-benzoyl-6-methyl-1*H*-indol-3-yl)-3,4,5-trimethoxybenzamide (**8**). Yield, 79.5%; mp: 250.1–250.7°C; ¹H NMR (400 MHz, DMSO-*d*₆) δ: 2.44 (s, 3H, CH₃), 3.71 (s, 3H, CH₃O), 3.78 (s, 6H, 2×CH₃O), 6.90 (s, 2H, ArH), 6.96 (d, *J* = 8.4 Hz, 1H, ArH), 7.28 (s, 1H, ArH), 7.42 (t, *J* = 14.8 Hz, 2H, ArH), 7.49 (d, *J* = 7.2 Hz, 1H, ArH), 7.55 (d, *J* = 8.4 Hz, 1H, ArH), 10.01 (s, 1H, NH), 11.65 (s, 1H, NH). ¹³C NMR (100 MHz, DMSO-*d*₆) δ: 187.98, 165.38, 152.78, 140.38, 138.77, 136.84, 135.82, 132.32, 129.30, 122.48, 121.81, 119.93, 112.49, 105.27, 60.48, 56.35, 22.08. HRMS (ESI) *m/z*: calcd for C₂₆H₂₄N₂O₅ (M+H⁺) 445.1685 found 445.1847.

5.1.4 *N*-(2-(4-chlorobenzoyl)-6-methyl-1*H*-indol-3-yl)-3,4,5-trimethoxybenzamide (**9**). Yield, 77.7%; mp: 252.2–252.8°C; ¹H NMR (400 MHz, DMSO-*d*₆) δ: 2.44 (s, 3H, CH₃), 3.70 (s, 3H, CH₃O), 3.80 (s, 6H, 2×CH₃O), 6.90 (s, 2H, ArH), 6.96 (d, *J* = 8.4 Hz, 1H, ArH), 7.27 (d, 1H, ArH),

215 7.46 (s, $J = 8.4$ Hz, 2H, ArH), 7.55 (d, $J = 8.0$ Hz, 2H, ArH), 7.72 (d, $J = 8.4$ Hz, 2H, ArH), 10.00 (s, 1H, NH), 11.70 (s, 1H, NH). ^{13}C NMR (100 MHz, DMSO- d_6) δ : 186.82, 165.49, 152.82, 140.43, 137.55, 136.96, 136.07, 131.03, 129.72, 128.56, 127.00, 122.62, 121.66, 120.04, 112.50, 105.19, 60.45, 56.30, 22.09. HRMS (ESI) m/z : calcd for $\text{C}_{26}\text{H}_{23}\text{ClN}_2\text{O}_5$ ($\text{M}+\text{H}^+$) 479.1295 found 479.1403.

220 5.1.5 *N*-(2-(biphenylcarbonyl)-6-methyl-1*H*-indol-3-yl)-3,4,5-trimethoxybenzamide (**10**). Yield, 83.0%; mp: 267.2–267.6°C; ^1H NMR (400 MHz, DMSO- d_6) δ : 2.45 (s, 3H, CH_3), 3.61 (s, 3H, CH_3O), 3.70 (s, 6H, $2\times\text{CH}_3\text{O}$), 6.96 (d, $J = 12.4$ Hz, 3H, ArH), 7.29 (s, 1H, ArH), 7.39–7.46 (m, 3H, ArH), 7.55 (dd, $J_1 = 7.6$ Hz, $J_2 = 8.8$ Hz, 3H, ArH), 7.67 (d, $J = 7.6$ Hz, 2H, ArH), 7.84 (d, $J = 8.0$ Hz, 2H, ArH), 10.02 (s, 1H, NH), 11.70 (s, 1H, NH). ^{13}C NMR (100 MHz, DMSO- d_6) δ : 187.51, 165.42, 152.75, 139.54, 137.63, 136.88, 135.88, 129.99, 129.36, 128.54, 127.28, 127.12, 126.71, 122.53, 122.02, 120.08, 105.29, 60.36, 56.21, 22.09. HRMS (ESI) m/z : calcd for $\text{C}_{32}\text{H}_{28}\text{N}_2\text{O}_5$ ($\text{M}+\text{H}^+$) 521.1998 found 521.2107.

230 5.1.6 3,4,5-trimethoxy-*N*-(6-methyl-2-(thiophene-2-carbonyl)-1*H*-indol-3-yl)benzamide (**11**). Yield, 69.0%; mp: 244.2–244.5°C; ^1H NMR (400 MHz, DMSO- d_6) δ : 3.73 (s, 3H, CH_3O), 3.83 (s, 6H, $2\times\text{CH}_3\text{O}$), 7.14 (d, $J = 6.0$ Hz, 2H, ArH), 7.19 (t, $J = 8.4$ Hz, 2H, ArH), 7.51 (s, 1H, ArH), 7.73 (d, $J = 8.4$ Hz, 1H, ArH), 7.84 (d, $J = 3.6$ Hz, 1H, ArH), 8.04 (d, $J = 4.8$ Hz, 1H, ArH), 10.32 (s, 1H, NH), 11.95 (s, 1H, NH). ^{13}C NMR (100 MHz, DMSO- d_6) δ : 179.28, 165.44, 153.00, 143.45, 140.68, 136.16, 135.34, 134.30, 130.41, 129.70, 128.78, 123.78, 122.30, 120.95, 119.03, 112.47, 105.47, 60.52, 56.43. HRMS (ESI) m/z : calcd for $\text{C}_{23}\text{H}_{19}\text{ClN}_2\text{O}_5\text{S}$ ($\text{M}+\text{H}^+$) 471.1093 found 471.0816.

235 5.1.7 *N*-(2-(2-naphthoyl)-6-methyl-1*H*-indol-3-yl)-3,4,5-trimethoxybenzamide (**12**). Yield, 79.7%; mp: 257.7–258.8°C; ^1H NMR (400 MHz, DMSO- d_6) δ : 2.44 (s, 3H, CH_3), 3.68 (s, 9H, $3\times\text{CH}_3\text{O}$), 6.70 (s, 2H, ArH), 6.95 (d, $J = 8.0$ Hz, 1H, ArH), 7.28 (s, 1H, ArH), 7.45 (t, $J = 15.2$ Hz, 1H, ArH), 7.55–7.59 (m, 3H, ArH), 7.73 (d, $J = 6.8$ Hz, 1H, ArH), 7.93–7.87 (m, 2H, ArH), 8.16 (d, $J = 8.0$ Hz, 1H, ArH), 9.93 (s, 1H, NH), 11.68 (s, 1H, NH). ^{13}C NMR (100 MHz, DMSO- d_6) δ : 188.68, 165.37, 152.65, 140.35, 136.34, 133.66, 131.25, 129.65, 128.54, 127.90, 127.29, 126.55, 125.11, 122.60, 121.24, 112.57, 105.13, 60.47, 56.22, 22.12. HRMS (ESI) m/z : calcd for $\text{C}_{30}\text{H}_{26}\text{N}_2\text{O}_5$ ($\text{M}+\text{H}^+$) 495.1842 found 495.1947.

240 5.1.8 *N*-(2-(4-fluorobenzoyl)-1*H*-indol-3-yl)-3,4,5-trimethoxybenzamide (**13**). Yield, 88.3%; mp: 255.2–255.9°C; ^1H NMR (400 MHz, DMSO- d_6) δ : 3.70 (s, 3H, CH_3O), 3.79 (s, 6H, $2\times\text{CH}_3\text{O}$), 6.92 (s, 2H, ArH), 7.12 (t, $J = 14.8$ Hz, 1H, ArH), 7.26 (t, $J = 16.0$ Hz, 2H, ArH), 7.35 (t, $J = 15.2$ Hz, 1H, ArH), 7.50 (d, $J = 8.4$ Hz, 1H, ArH), 7.65 (d, $J = 8.4$ Hz, 1H, ArH), 7.81–7.84 (m, 2H, ArH), 10.03 (s, 1H, NH), 11.84 (s, 1H, NH). ^{13}C NMR (100 MHz, DMSO- d_6) δ : 186.85, 165.62, 152.80, 140.48, 137.43, 137.06, 136.46, 131.15, 130.67, 129.51, 128.62, 128.23, 123.57, 122.65, 121.01, 119.51, 112.48, 105.30, 60.45, 56.33. HRMS (ESI) m/z : calcd for $\text{C}_{25}\text{H}_{21}\text{FN}_2\text{O}_5$ ($\text{M}+\text{H}^+$) 448.1434 found 448.1577.

250 5.1.9 3,4,5-trimethoxy-N-(2-(4-methylbenzoyl)-1H-indol-3-yl)benzamide (**14**). Yield, 75.3%; mp: 241.5–241.8°C; ¹H NMR (400 MHz, DMSO-d₆) δ: 2.26 (s, 3H, CH₃), 3.70 (s, 3H, CH₃O), 3.78 (s, 6H, 2×CH₃O), 6.92 (s, 2H, ArH), 7.12 (d, *J* = 7.2 Hz, 1H, ArH), 7.28 (d, *J* = 7.6 Hz, 2H, ArH), 7.33 (t, *J* = 14.8 Hz, 2H, ArH), 7.50 (d, *J* = 6.6 Hz, 1H, ArH), 7.64 (d, *J* = 8.0 Hz, 1H, ArH), 7.69 (d, *J* = 7.6 Hz, 2H, ArH), 10.00 (s, 1H, NH), 11.77 (s, 1H, NH). ¹³C NMR (100 MHz, DMSO-d₆) δ: 187.83, 165.54, 152.78, 142.67, 140.37, 136.12, 135.95, 129.92, 127.85, 125.86, 123.94, 121.86, 120.26, 119.23, 113.10, 105.32, 60.46, 56.32, 21.42. HRMS (ESI) *m/z*: calcd for C₂₆H₂₄N₂O₅ (M+H⁺) 445.1685 found 445.1888.

260 5.1.10 N-(2-benzoyl-1H-indol-3-yl)-3,4,5-trimethoxybenzamide (**15**). Yield, 74.5%; mp: 248.6–248.9°C; ¹H NMR (400 MHz, DMSO-d₆) δ: 3.70 (s, 3H, CH₃O), 3.78 (s, 6H, 2×CH₃O), 6.90 (s, 2H, ArH), 7.12 (t, *J* = 14.8 Hz, 1H, ArH), 7.34 (t, *J* = 15.2 Hz, 1H, ArH), 7.43 (t, *J* = 14.8 Hz, 2H, ArH), 7.51 (d, *J* = 8.4 Hz, 2H, ArH), 7.65 (d, *J* = 8.0 Hz, 1H, ArH), 10.02 (s, 1H, NH), 11.80 (s, 1H, NH). ¹³C NMR (100 MHz, DMSO-d₆) δ: 188.14, 165.52, 152.77, 138.59, 136.24, 132.48, 129.87, 129.36, 129.14, 128.73, 128.51, 127.71, 126.01, 123.90, 121.88, 119.42, 105.28, 60.48, 56.36. HRMS (ESI) *m/z*: calcd for C₂₅H₂₂N₂O₅ (M+H⁺) 431.1529 found 431.1704.

265 5.1.11 N-(2-(4-bromobenzoyl)-1H-indol-3-yl)-3,4,5-trimethoxybenzamide (**16**). Yield, 81.0%; mp: 253.3–253.8°C; ¹H NMR (400 MHz, DMSO-d₆) δ: 3.72 (s, 3H, CH₃O), 3.81 (s, 6H, 2×CH₃O), 6.91 (s, 2H, ArH), 7.13 (t, *J* = 15.2 Hz, 1H, ArH), 7.36 (t, *J* = 15.2 Hz, 2H, ArH), 7.50 (d, *J* = 8.4 Hz, 1H, ArH), 7.61 (d, *J* = 7.6 Hz, 2H, ArH), 7.67 (d, *J* = 7.6 Hz, 3H, ArH), 10.01 (s, 1H, NH), 11.85 (s, 1H, NH). ¹³C NMR (100 MHz, DMSO-d₆) δ: 187.17, 165.63, 152.82, 140.43, 137.70, 136.36, 131.52, 131.20, 129.71, 127.52, 126.25, 123.90, 121.76, 120.44, 119.59, 113.16, 105.18, 60.45, 56.32. HRMS (ESI) *m/z*: calcd for C₂₅H₂₁BrN₂O₅ (M+H⁺) 509.0634 found 509.10735.

275 5.1.12 N-(2-(biphenylcarbonyl)-1H-indol-3-yl)-3,4,5-trimethoxybenzamide (**17**). Yield, 74.3%; mp: 266.6–267.1°C; ¹H NMR (400 MHz, DMSO-d₆) δ: 3.61 (s, 3H, CH₃O), 3.70 (s, 6H, 2×CH₃O), 6.94 (s, 2H, ArH), 7.13 (t, *J* = 14.8 Hz, 1H, ArH), 7.35–7.47 (m, 4H, ArH), 7.53 (t, *J* = 16.4 Hz, 3H, ArH), 7.64–7.69 (m, 2H, ArH), 7.85 (d, *J* = 8.0 Hz, 2H, ArH), 10.02 (s, 1H, NH), 11.84 (s, 1H, NH). ¹³C NMR (100 MHz, DMSO-d₆) δ: 187.68, 165.55, 152.75, 139.51, 137.45, 136.27, 130.05, 129.80, 129.38, 128.58, 127.86, 127.14, 126.74, 124.03, 119.58, 113.16, 105.31, 60.37, 56.22. HRMS (ESI) *m/z*: calcd for C₃₁H₂₆N₂O₅ (M+H⁺) 507.1842 found 507.1927.

280 5.1.13 3,4,5-trimethoxy-N-(2-(3-methoxybenzoyl)-1H-indol-3-yl)benzamide (**18**). Yield, 70.0%; mp: 256.1–256.6°C; ¹H NMR (400 MHz, DMSO-d₆) δ: 3.71 (d, *J* = 6.8 Hz, 6H, 2×CH₃O), 3.78 (s, 6H, 2×CH₃O), 6.91 (s, 2H, ArH), 7.02–7.12 (m, 2H, ArH), 7.26 (s, 1H, ArH), 7.33 (d, *J* = 8.0 Hz, 2H, ArH), 7.50 (d, *J* = 8.4 Hz, 1H, ArH), 7.67 (d, *J* = 8.0 Hz, 1H, ArH), 10.13 (s, 1H, NH), 11.82 (s, 1H,

NH). ^{13}C NMR (100 MHz, DMSO- d_6) δ : 187.76, 165.49, 159.24, 152.80, 139.68, 136.37, 130.59, 129.78, 129.61, 123.75, 122.57, 121.64, 118.88, 113.79, 112.46, 105.23, 60.50, 56.30, 55.48.

285 HRMS (ESI) m/z : calcd for $\text{C}_{26}\text{H}_{24}\text{N}_2\text{O}_6$ ($\text{M}+\text{H}^+$) 461.1634 found 461.1855.

5.1.14 *3,4,5-trimethoxy-N-(2-(thiophene-2-carbonyl)-1H-indol-3-yl)benzamide (19)*. Yield, 80.1%; mp: 245.2–246.0°C; ^1H NMR (400 MHz, DMSO- d_6) δ : 3.73 (s, 3H, CH_3O), 3.83 (s, 6H, $2\times\text{CH}_3\text{O}$), 7.14 (d, $J = 5.2$ Hz, 3H, ArH), 7.20 (t, $J = 8.4$ Hz, 1H, ArH), 7.35 (t, $J = 15.2$ Hz, 1H, ArH), 7.50 (d, $J = 8.0$ Hz, 1H, ArH), 7.70 (d, $J = 8.0$ Hz, 1H, ArH), 7.86 (d, $J = 7.2$ Hz, 1H, ArH), 8.02 (d, $J = 4.8$ Hz, 1H, ArH), 10.28 (s, 1H, NH), 11.79 (s, 1H, NH). ^{13}C NMR (100 MHz, DMSO- d_6) δ : 179.45, 165.46, 152.99, 143.70, 136.06, 135.05, 134.18, 129.91, 128.72, 125.88, 123.61, 122.03, 119.11, 113.15, 105.45, 60.51, 56.42. HRMS (ESI) m/z : calcd for $\text{C}_{23}\text{H}_{20}\text{N}_2\text{O}_5\text{S}$ ($\text{M}+\text{H}^+$) 437.1093 found 437.1213.

290

5.1.15 *3,4,5-trimethoxy-N-(2-(4-methoxybenzoyl)-1H-indol-3-yl)benzamide (20)*. Yield, 64.9%; mp: 256.0–256.7°C; ^1H NMR (400 MHz, DMSO- d_6) δ : 3.72 (d, $J = 3.2$ Hz, 6H, $2\times\text{CH}_3\text{O}$), 3.78 (s, 6H, $2\times\text{CH}_3\text{O}$), 6.94 (s, 1H, ArH), 6.96 (s, 3H, ArH), 7.12 (d, $J = 8.4$ Hz, 1H, ArH), 7.33 (t, $J = 15.2$ Hz, 1H, ArH), 7.49 (d, $J = 8.0$ Hz, 1H, ArH), 7.63 (d, $J = 8.0$ Hz, 1H, ArH), 7.79 (d, $J = 8.4$ Hz, 2H, ArH), 10.00 (s, 1H, NH), 11.75 (s, 1H, NH). ^{13}C NMR (100 MHz, DMSO- d_6) δ : 186.80, 165.59, 162.96, 152.81, 140.39, 135.99, 131.79, 131.11, 129.99, 128.03, 125.66, 124.01, 121.78, 120.21, 118.71, 113.93, 113.05, 105.35, 60.48, 56.30, 55.81. HRMS (ESI) m/z : calcd for $\text{C}_{26}\text{H}_{24}\text{N}_2\text{O}_6$ ($\text{M}+\text{H}^+$) 461.1634 found 461.1858.

295

300

5.1.16 *N-(6-chloro-2-(4-fluorobenzoyl)-1H-indol-3-yl)-3,4,5-trimethoxybenzamide (21)*. Yield, 76.2%; mp: 254.1–254.6°C; ^1H NMR (400 MHz, DMSO- d_6) δ : 3.71 (s, 3H, CH_3O), 3.79 (s, 6H, $2\times\text{CH}_3\text{O}$), 6.92 (s, 2H, ArH), 7.16 (d, $J = 8.8$ Hz, 1H, ArH), 7.26 (t, $J = 15.6$ Hz, 2H, ArH), 7.51 (s, 1H, ArH), 7.69 (d, $J = 8.8$ Hz, 1H, ArH), 7.83 (dd, $J_1 = 5.6$ Hz, $J_2 = 5.6$ Hz, 2H, ArH), 10.08 (s, 1H, NH), 11.98 (s, 1H, NH). ^{13}C NMR (100 MHz, DMSO- d_6) δ : 186.85, 165.62, 152.83, 140.53, 136.36, 132.20, 132.11, 129.57, 128.26, 123.53, 122.57, 121.00, 119.26, 115.73, 115.51, 105.27, 60.49, 56.34. HRMS (ESI) m/z : calcd for $\text{C}_{25}\text{H}_{20}\text{ClFN}_2\text{O}_5$ ($\text{M}+\text{H}^+$) 483.1045 found 483.1143.

305

5.1.17 *N-(6-chloro-2-(4-methylbenzoyl)-1H-indol-3-yl)-3,4,5-trimethoxybenzamide (22)*. Yield, 74.6 %; mp: 255.7–256.5°C; ^1H NMR (400 MHz, DMSO- d_6) δ : 2.26 (s, 3H, CH_3), 3.70 (s, 3H, CH_3O), 3.78 (s, 6H, $2\times\text{CH}_3\text{O}$), 6.91 (s, 2H, ArH), 7.14 (d, $J = 8.4$ Hz, 1H, ArH), 7.23 (d, $J = 7.6$ Hz, 2H, ArH), 7.50 (s, 1H, ArH), 7.68 (d, $J = 8.0$ Hz, 3H, ArH), 10.05 (s, 1H, NH), 11.92 (s, 1H, NH). ^{13}C NMR (100 MHz, DMSO- d_6) δ : 187.67, 165.57, 152.86, 142.98, 140.52, 136.20, 135.73, 129.60, 129.20, 127.85, 123.69, 122.65, 120.83, 119.21, 112.47, 105.39, 60.52, 56.38, 21.43. HRMS (ESI) m/z : calcd for $\text{C}_{26}\text{H}_{23}\text{ClN}_2\text{O}_5$ ($\text{M}+\text{H}^+$) 479.1295 found 479.1388.

310

315

5.1.18 *N-(6-chloro-2-benzoyl-1H-indol-3-yl)-3,4,5-trimethoxybenzamide (23)*. Yield, 85.1%; mp:

259.2–259.9°C; ¹H NMR (400 MHz, DMSO-d₆) δ: 3.70 (s, 3H, CH₃O), 3.77 (s, 6H, 2×CH₃O), 6.89 (s, 2H, ArH), 7.15 (d, *J* = 8.8 Hz, 1H, ArH), 7.43 (t, *J* = 15.2 Hz, 2H, ArH), 7.52 (d, *J* = 6.0 Hz, 2H, ArH), 7.69 (d, *J* = 8.8 Hz, 1H, ArH), 7.78 (d, *J* = 7.6 Hz, 2H, ArH), 10.07 (s, 1H, NH), 11.95 (s, 1H, NH). ¹³C NMR (100 MHz, DMSO-d₆) δ: 186.85, 165.52, 152.83, 140.53, 136.36, 132.20, 132.11, 130.61, 129.57, 128.26, 123.53, 122.57, 121.00, 119.26, 115.73, 115.51, 111.24, 105.27, 60.49, 56.34. HRMS (ESI) *m/z*: calcd for C₂₅H₂₁ClN₂O₅ (M+H⁺) 465.1139 found 465.1256.

5.1.19 *N*-(6-chloro-2-(4-methoxybenzoyl)-1*H*-indol-3-yl)-3,4,5-trimethoxybenzamide (**24**). Yield, 87.0%; mp: 256.0–256.6°C; ¹H NMR (400 MHz, DMSO-d₆) δ: 3.72 (d, *J* = 4.4 Hz, 6H, 2×CH₃O), 3.78 (s, 6H, 2×CH₃O), 6.96 (t, *J* = 8.4 Hz, 4H, ArH), 7.14 (d, *J* = 8.8 Hz, 1H, ArH), 7.51 (s, 1H, ArH), 7.67 (d, *J* = 8.4 Hz, 1H, ArH), 7.79 (d, *J* = 8.4 Hz, 2H, ArH), 10.05 (s, 1H, NH), 11.91 (s, 1H, NH). ¹³C NMR (100 MHz, DMSO-d₆) δ: 186.61, 165.55, 163.06, 152.82, 140.48, 136.13, 131.82, 130.83, 130.21, 129.77, 128.67, 123.54, 122.70, 120.82, 118.71, 113.99, 112.38, 105.38, 60.48, 56.31, 55.83. HRMS (ESI) *m/z*: calcd for C₂₆H₂₃ClN₂O₆ (M+H⁺) 495.1245 found 495.1353.

5.1.20 *N*-(6-chloro-2-(3-methoxybenzoyl)-1*H*-indol-3-yl)-3,4,5-trimethoxybenzamide (**25**). Yield, 65.3%; mp: 254.2–254.7°C; ¹H NMR (400 MHz, DMSO-d₆) δ: 3.71 (d, *J* = 2.4 Hz, 6H, 2×CH₃O), 3.78 (s, 6H, 2×CH₃O), 6.91 (s, 2H, ArH), 7.07 (d, *J* = 4.8 Hz, 1H, ArH), 7.14 (d, *J* = 8.8 Hz, 1H, ArH), 7.26 (s, 1H, ArH), 7.34 (d, *J* = 4.8 Hz, 2H, ArH), 7.51 (s, 1H, ArH), 7.67 (d, *J* = 8.8 Hz, 1H, ArH), 10.07 (s, 1H, NH), 11.96 (s, 1H, NH). ¹³C NMR (100 MHz, DMSO-d₆) δ: 187.76, 165.49, 159.24, 152.80, 139.68, 136.37, 130.59, 129.78, 129.61, 123.75, 122.57, 121.64, 118.88, 113.79, 112.46, 105.23, 60.50, 56.30, 55.48. HRMS (ESI) *m/z*: calcd for C₂₆H₂₃ClN₂O₆ (M+H⁺) 495.1245 found 495.1353.

5.1.21 *N*-(6-chloro-2-(3-bromobenzoyl)-1*H*-indol-3-yl)-3,4,5-trimethoxybenzamide (**26**). Yield, 65.4%; mp: 241.2–241.9°C; ¹H NMR (400 MHz, DMSO-d₆) δ: 3.70 (s, 3H, CH₃O), 3.79 (s, 6H, 2×CH₃O), 6.95 (s, 2H, ArH), 7.14 (d, *J* = 8.4 Hz, 1H, ArH), 7.36 (t, *J* = 15.2 Hz, 1H, ArH), 7.52 (s, 1H, ArH), 7.70 (dd, *J*₁ = 8.4 Hz, *J*₂ = 12.4 Hz, 3H, ArH), 7.85 (s, 1H, ArH), 10.27 (s, 1H, NH), 12.05 (s, 1H, NH). ¹³C NMR (100 MHz, DMSO-d₆) δ: 187.76, 165.49, 159.24, 152.80, 139.68, 136.37, 130.59, 129.78, 129.61, 123.75, 122.57, 121.64, 120.95, 119.53, 118.88, 113.79, 112.46, 105.23, 60.50, 56.30. HRMS (ESI) *m/z*: calcd for C₂₅H₂₀ClBrN₂O₅ (M+H⁺) 543.0244 found 543.0329.

5.1.22 *N*-(6-chloro-2-(4-chlorobenzoyl)-1*H*-indol-3-yl)-3,4,5-trimethoxybenzamide (**27**). Yield, 67.8%; mp: 248.1–248.9°C; ¹H NMR (400 MHz, DMSO-d₆) δ: 3.71 (s, 3H, CH₃O), 3.80 (s, 6H, 2×CH₃O), 6.93 (s, 2H, ArH), 7.14 (d, *J* = 8.8 Hz, 1H, ArH), 7.46 (d, *J* = 8.0 Hz, 2H, ArH), 7.53 (s, 1H, ArH), 7.70 (d, *J* = 8.8 Hz, 1H, ArH), 7.75 (d, *J* = 8.0 Hz, 2H, ArH), 10.20 (s, 1H, NH), 12.03 (s, 1H, NH). ¹³C NMR (100 MHz, DMSO-d₆) δ: 186.85, 165.62, 152.80, 140.48, 137.33, 137.06, 136.46, 131.15, 130.67, 129.51, 128.62, 128.23, 123.57, 122.57, 121.01, 119.51, 105.30, 60.45,

56.33. HRMS (ESI) m/z : calcd for $C_{25}H_{20}Cl_2N_2O_5$ ($M+H^+$) 499.0749 found 499.0849.

355 5.1.21 *N*-(6-chloro-2-(furan-2-carbonyl)-1*H*-indol-3-yl)-3,4,5-trimethoxybenzamide (**28**). Yield, 62.7%; mp: 241.2–241.8°C; 1H NMR (400 MHz, DMSO- d_6) δ : 3.75 (s, 3H, CH₃O), 3.85 (s, 6H, 2×CH₃O), 6.95 (s, 1H, ArH), 7.15 (d, J = 8.8 Hz, 1H, ArH), 7.24 (s, 2H, ArH), 7.42 (s, 1H, ArH), 7.54 (s, 1H, ArH), 7.81 (d, J = 8.8 Hz, 1H, ArH), 8.03 (s, 1H, ArH), 10.52 (s, 1H, NH), 11.87 (s, 1H, NH). ^{13}C NMR (100 MHz, DMSO- d_6) δ : 165.62, 153.09, 152.01, 140.80, 140.48, 136.41, 130.70, 129.86, 126.62, 124.29, 121.64, 120.87, 120.47, 119.81, 113.14, 112.54, 105.55, 60.54, 56.48. HRMS (ESI) m/z : calcd for $C_{23}H_{19}ClN_2O_6$ ($M+H^+$) 455.0932 found 455.1026.

360 5.1.22 *N*-(6-chloro-2-(thiophene-2-carbonyl)-1*H*-indol-3-yl)-3,4,5-trimethoxybenzamide (**29**). Yield, 66.0%; mp: 244.2–244.5°C; 1H NMR (400 MHz, DMSO- d_6) δ : 3.73 (s, 3H, CH₃O), 3.83 (s, 6H, 2×CH₃O), 7.14(d, J = 6.0 Hz, 2H, ArH), 7.19 (t, J = 8.4 Hz, 2H, ArH), 7.51 (s, 1H, ArH), 7.73 (d, J = 8.4 Hz, 1H, ArH), 7.84 (d, J = 3.6 Hz, 1H, ArH), 8.04 (d, J = 4.8 Hz, 1H, ArH), 10.32 (s, 1H, NH), 11.95 (s, 1H, NH). ^{13}C NMR (100 MHz, DMSO- d_6) δ : 179.28, 165.44, 153.00, 143.45, 140.68, 136.16, 135.34, 134.30, 130.41, 129.70, 128.78, 123.78, 122.30, 120.95, 119.03, 112.47, 105.47, 60.52, 56.43. HRMS (ESI) m/z : calcd for $C_{23}H_{19}ClN_2O_5S$ ($M+H^+$) 471.1093 found 471.0816.

370 5.1.21 *N*-(6-chloro-2-(3,4-difluorobenzoyl)-1*H*-indol-3-yl)-3,4,5-trimethoxybenzamide (**30**). Yield, 76.8%; mp: 254.3–254.8°C; 1H NMR (400 MHz, DMSO- d_6) δ : 3.72 (s, 3H, CH₃O), 3.80 (s, 6H, 2×CH₃O), 6.96 (s, 2H, ArH), 7.16 (dd, J_1 = 0.4 Hz, J_2 = 0.4 Hz, 1H, ArH), 7.47-7.52 (m, 2H, ArH), 7.60 (s, 1H, ArH), 7.74 (dd, J_1 = 0.8 Hz, J_2 = 0.8 Hz, 2H, ArH), 10.15 (s, 1H, NH), 12.04 (s, 1H, NH). ^{13}C NMR (100 MHz, DMSO- d_6) δ : 185.54, 165.62, 152.87, 140.66, 136.53, 130.90, 129.34, 127.88, 123.48, 122.53, 121.15, 119.61, 118.68, 118.50, 117.94, 117.76, 112.49, 105.21, 60.51, 56.30. HRMS (ESI) m/z : calcd for $C_{25}H_{19}ClF_2N_2O_5$ ($M+H^+$) 501.0951 found 501.1049.

375 5.1.22 *N*-(6-chloro-2-(3-hydroxy-4-methoxybenzoyl)-1*H*-indol-3-yl)-3,4,5-trimethoxybenzamide (**31**). Yield, 54.5%; mp: 247.7–248.0°C; 1H NMR (400 MHz, DMSO- d_6) δ : 3.72 (d, J = 4.4 Hz, 6H, 2×CH₃O), 3.79 (s, 6H, 2×CH₃O), 6.89 (d, J = 8.8 Hz, 1H, ArH), 6.98 (s, 2H, ArH), 7.14 (dd, J_1 = 2.0 Hz, J_2 = 1.6 Hz, 1H, ArH), 7.29 (d, J = 6.8 Hz, 2H, ArH), 7.49 (d, J = 1.6 Hz, 1H, ArH), 7.68 (d, J = 8.8 Hz, 1H, ArH), 10.06 (s, 1H, NH), 11.84 (s, 1H, NH). ^{13}C NMR (100 MHz, DMSO- d_6) δ : 186.76, 165.54, 158.62, 152.84, 152.00, 146.66, 140.45, 136.01, 131.02, 129.97, 128.48, 123.62, 122.52, 120.72, 118.72, 116.04, 112.33, 114.45, 105.37, 60.48, 56.30, 56.08. HRMS (ESI) m/z : calcd for $C_{27}H_{26}N_2O_8$ ($M+K^+$) 544.1689 found 544.4191.

385 5.1.22 3,4,5-trimethoxy-*N*-(6-methoxy-2-(4-methoxybenzoyl)-1*H*-indol-3-yl)benzamide (**32**). Yield, 86.0%; mp: 258.8–259.7°C; 1H NMR (400 MHz, DMSO- d_6) δ : 3.72 (s, 6H, 2×CH₃O), 3.79 (s, 6H, 2×CH₃O), 3.83 (s, 3H, CH₃O), 6.77 (dd, J_1 = 1.6 Hz, J_2 = 2.0 Hz, 1H, ArH), 6.91-6.95 (m, 3H, ArH), 6.98 (s, 2H, ArH), 7.57 (d, J = 8.8 Hz, 1H, ArH), 7.76 (d, J = 8.4 Hz, 2H, ArH), 10.08 (s, 1H,

NH), 11.55 (s, 1H, NH). ^{13}C NMR (100 MHz, DMSO- d_6) δ : 186.22, 165.33, 162.66, 159.04, 152.84, 137.47, 131.88, 131.41, 129.93, 126.63, 123.32, 120.32, 120.32, 118.13, 112.21, 105.36, 60.49, 56.31, 55.77, 55.62. HRMS (ESI) m/z : calcd for $\text{C}_{27}\text{H}_{26}\text{N}_2\text{O}_7$ ($\text{M}+\text{H}^+$) 491.1740 found 491.1912.

390 5.1.21 3,4,5-trimethoxy-*N*-(6-methoxy-2-benzoyl-1*H*-indol-3-yl)benzamide (**33**). Yield, 84.2%; mp: 259.3–259.6°C; ^1H NMR (400 MHz, DMSO- d_6) δ : 3.71 (s, 3H, CH_3O), 3.79 (s, 6H, $2\times\text{CH}_3\text{O}$), 3.83 (s, 3H, CH_3O), 6.77 (dd, $J_1 = 1.6$ Hz, $J_2 = 2.0$ Hz, 1H, ArH), 6.91–6.93 (m, 3H, ArH), 7.43 (t, $J = 14.8$ Hz, 2H, ArH), 7.50 (d, $J = 7.2$ Hz, 1H, ArH), 7.60 (d, $J = 9.2$ Hz, 1H, ArH), 10.11 (s, 1H, NH), 11.59 (s, 1H, NH). ^{13}C NMR (100 MHz, DMSO- d_6) δ : 187.43, 165.29, 159.29, 152.82, 140.47, 138.94, 137.79, 132.15, 129.81, 129.20, 128.49, 126.34, 123.47, 121.11, 118.00, 112.34, 105.30, 94.12, 60.50, 56.37, 55.63. HRMS (ESI) m/z : calcd for $\text{C}_{26}\text{H}_{24}\text{N}_2\text{O}_6$ ($\text{M}+\text{H}^+$) 461.1634 found 461.1740.

400 5.1.22 3,4,5-trimethoxy-*N*-(6-methoxy-2-(4-methylbenzoyl)-1*H*-indol-3-yl)benzamide (**34**). Yield, 88.9%; mp: 253.2–253.7°C; ^1H NMR (400 MHz, DMSO- d_6) δ : 2.27 (s, 3H, CH_3), 3.71 (s, 3H, CH_3O), 3.80 (s, 6H, $2\times\text{CH}_3\text{O}$), 3.83 (s, 3H, CH_3O), 6.77 (dd, $J_1 = 2.0$ Hz, $J_2 = 0.8$ Hz, 1H, ArH), 6.91 (d, $J = 1.6$ Hz, 1H, ArH), 6.96 (s, 2H, ArH), 7.22 (d, $J = 8.0$ Hz, 2H, ArH), 7.59 (d, $J = 8.8$ Hz, 1H, ArH), 7.66 (d, $J = 8.0$ Hz, 2H, ArH), 10.09 (s, 1H, NH), 11.56 (s, 1H, NH). ^{13}C NMR (100 MHz, DMSO- d_6) δ : 187.17, 165.27, 159.18, 152.83, 142.26, 140.45, 137.66, 136.27, 129.85, 129.37, 129.06, 126.43, 123.47, 120.94, 118.01, 112.25, 105.33, 94.13, 60.47, 56.33, 55.62, 21.40. HRMS (ESI) m/z : calcd for $\text{C}_{27}\text{H}_{26}\text{N}_2\text{O}_6$ ($\text{M}+\text{H}^+$) 475.1791 found 475.1990.

405 5.2 Biological evaluation

5.2.1 Antitumor activity

The antitumor activities of compounds **6–34** were evaluated with MCF-7, MDA-MB-231, BT549, T47D, MDA-MB-468, and HS578T cell lines by the standard MTT (3-(4,5-dimethylthiazol-2-yl)-2,5-diphenyltetrazolium bromide) assay *in vitro*. The cancer cell lines were cultured in RPMI-1640 medium supplemented with 10% FBS. Tested compounds were prepared by dissolving in dimethyl sulfoxide (DMSO) at 100 mM and diluted with the medium into a series of concentrations. Exponentially growing cells were plated in 96-well plates (2×10^3 cells/well) and incubated at 37 °C for 24 h for attachment. The culture medium was then changed, and cells grew in medium with the tested compounds. DMSO (0.1%) and CA-4 were used as negative and positive control, respectively. Cells were incubated at 37 °C for 72 h. After the treatment period, 10 μL of MTT solution (5 mg/mL) was added to each well, and the plates were incubated for 4 h at 37°C. The medium was then aspirated and formazan crystals were dissolved in

DMSO (150 μ L) for about 10 mins. The absorbance at 570 nm (Abs) of the suspension was measured by a microplate reader (Bio-Rad laboratories, USA). The inhibition percentage was calculated using the following formula: % inhibition = $(Abs_{control} - Abs_{compound}) / Abs_{control} \times 100\%$. The IC₅₀ values of the tested compounds and CA-4 were measured by treating cells with drugs of various concentrations and analyzed by use of the prism statistical package (GraphPad Software, San Diego, CA, U.S.A.).

5.2.2 Flow-activating cell sorting (FACS) analysis

Flow cytometric analysis analysis was performed to estimate the effect of compound **27** on cell cycle phase distribution of human breast cancer cell lines (BT549). When the cells grew to about 70% confluence in 60 mm dishes over night, they were incubated with compound **27** at 2, 4, and 8 μ M concentrations for 24 h. Control and treated cells were harvested, washed with PBS, and fixed in 75% ice-cold ethanol at 4 $^{\circ}$ C overnight. They were then washed with PBS, incubated with 50 μ g/mL of RNase at 37 $^{\circ}$ C for 30 min, stained with 50 μ g/mL of propidium iodide, and then subjected to flow cytometry (Beckman Coulter).

5.2.3 Immunocytochemistry

BT549 cells (2×10^4 cells/well) were plated on glass coverslips in 12-well plates and allowed to attach overnight. After treatment with compound **27** (10 and 20 μ M) or 0.1% DMSO for 6 h, cells were rinsed twice, fixed with 4% paraformaldehyde, and permeabilized with 0.1% Triton X-100. After blocking with 5% BSA for 60 min, the coverslips were incubated overnight at 4 $^{\circ}$ C with primary antibodies (α -tubulin mouse monoclonal antibody and β -tubulin rabbit monoclonal antibody). After washing, the cells were incubated with the following secondary antibodies: Alexa Fluor[®] 555 conjugate anti-rabbit IgG and FITC AffiniPure goat anti-mouse IgG. Nuclei were visualized by inclusion of DAPI. Images were taken using a laser scanning confocal microscope (Carl Zeiss LSM 880).

5.2.4 In vitro tubulin polymerization assay

The *in vitro tubulin polymerization* activity assay was performed following our previously reported method [25].

5.2.5 Molecular modeling

Molecular docking simulation studies were carried out by using the SURFLEX module of

SYBYL 7.3 package [26], and the tubulin structure was down loaded from the PDB data bank (<http://www.rcsb.org/-PDB> code: 5lyj) [27]. The studied molecule was initially built in Sybyl 7.3. Structural energy minimization process was performed using the Tripos force field with a distance–dependent dielectric and powell gradient algorithm with a convergence criterion of 0.005 kcal/mol Å. Meanwhile, partial atomic charges were calculated using Gasteiger–Hückel method. The best of the 20 conformations with different scores were obtained. During the docking process, all the other parameters were assigned their default values. The best ranking pose was visualized with PyMOL [24].

Acknowledgments

We should thank Dr. Hong-Bing Zhao (Shanghai TANG Bioscience Co., Ltd.) for the test of tubulin polymerisation activity. The present work was supported by the National Natural Science Foundation of China (21372113), and the Science and Technology Program of Guangzhou, China (201707010198).

Appendix A. Supplementary data

Supplementary data related to this article can be found at <http://dx.doi.org/10.1016/j.ejmech.2018.xx.xxx>.

References

- [1] A. Muroyama, T. Lechler. Microtubule organization, dynamics and functions in differentiated cells. *Development*. 144 (2017) 3012–3021.
- [2] C. Dumontet, M.A. Jordan. Microtubule-binding agents: a dynamic field of cancer therapeutics. *Nat Rev Drug Discov*. 9 (2010) 790–803.
- [3] S. Chaaban, G.J. Brouhard. A microtubule bestiary: structural diversity in tubulin polymers. *Mol Biol Cell*. 28 (2017) 2924–2931.
- [4] S. Banerjee, K.E. Arnst, Y. Wang, G. Kumar, S. Deng, L. Yang, G.B. Li, J. Yang, S.W. White, W. Li, D.D. Miller. Heterocyclic-fused pyrimidines as novel tubulin polymerization inhibitors targeting the colchicine binding site: structural basis and antitumor efficacy. *J Med Chem*. 61 (2018) 1704–1718.
- [5] Y.N. Cao, L.L. Zheng, D. Wang, X.X. Liang, F. Gao, X.L. Zhou. Recent advances in microtubule-stabilizing agents. *Eur J Med Chem*. 143 (2018) 806–828.
- [6] A. Siddiqui-Jain, J.P. Hoj, D.W. Cescon, M.D. Hansen. Pharmacology and in vivo efficacy of pyridine-pyrimidine amides that inhibit microtubule polymerization. *Bioorg Med Chem Lett*. 28 (2018) 934–941.

- [7] R. Aguayo-Ortiz, L. Cano-González, R. Castillo, A. Hernández-Campos, L. Dominguez. Structure-based approaches for the design of benzimidazole-2-carbamate derivatives as tubulin polymerization inhibitors. *Chem Biol Drug Des.* 90 (2017) 40–51.
- [8] R. Patil, S.A.Patil, K.D.Beaman, S.A.Patil. Indole molecules as inhibitors of tubulin polymerization: potential new anticancer agents, an update (2013-2015). *Future Med Chem.* 8 (2016) 1291–316.
- [9] W. Li, H. Sun, S. Xu, Z. Zhu, J. Xu. Tubulin inhibitors targeting the colchicine binding site: a perspective of privileged structures. *Future Med Chem.* 9 (2017) 1765–1794.
- [10] B.G.M. Youssif, M.H. Abdelrahman, A.H. Abdelazeem, M.A. Abdelgawad, H.M. Ibrahim, O.I.A. Salem, M.F.A. Mohamed, L. Treambleau, S.N.A. Bukhari. Design, synthesis, mechanistic and histopathological studies of small-molecules of novel indole-2-carboxamides and pyrazino[1,2-a]indol-1(2H)-ones as potential anticancer agents effecting the reactive oxygen species production. *Eur J Med Chem.* 146 (2018) 260–273.
- [11] D.W. Carney, J.C. 3rd Lukesh, D.M. Brody, M.M. Brütsch, D.L. Boger. Ultrapotent vinblastines in which added molecular complexity further disrupts the target tubulindimer-dimer interface. *Proc Natl Acad Sci U S A.* 113 (2016) 9691–9698.
- [12] K.C. Feng, Y.R. Liang, P.F. Zhou, M.M. Liu, Y. Wang. Structural modification and inhibitory activity on tumor cell proliferation of novel diaryl- β -lactam compounds as tubulin aggregation inhibitors. *Chin J Org Chem.* 37 (2017) 683–690.
- [13] P. Liu, Y. Qin, L. Wu, S. Yang, N. Li, H. Wang, H. Xu, K. Sun, S. Zhang, X. Han, Y. Sun, Y. Shi. A phase I clinical trial assessing the safety and tolerability of combretastatin A4 phosphate injections. *Anticancer Drugs.* 25 (2014) 462–471.
- [14] A. Brancale, R.Silvestri. Indole, a core nucleus for potent inhibitors of tubulin polymerization. *Med Res Rev.* 27 (2007) 209–238.
- [15] G. La Regina, R. Bai, A. Coluccia, et al. New indole tubulin assembly inhibitors cause stable arrest of mitotic progression, enhanced stimulation of natural killer cell cytotoxic activity, and repression of hedgehog-dependent cancer. *J Med Chem.* 58 (2015) 5789–5807.
- [16] G. La Regina, T. Sarkar, R. Bai, M.C. Edler, R. Saletti, A. Coluccia, F. Piscitelli, L. Minelli, V. Gatti, C. Mazzocoli, V. Palermo, C. Mazzoni, C. Falcone, A.I. Scovassi, V. Giansanti, P. Campiglia, A. Porta, B. Maresca, E. Hamel, A. Brancale, E. Novellino, R. Silvestri. New arylthioindoles and related bioisosteres at the sulfur bridging group. 4. Synthesis, tubulin polymerization, cell growth inhibition, and molecular modeling studies. *J Med Chem.* 52 (2009) 7512–7527.
- [17] M.T. Macdonough, T.E. Strecker, E. Hamel, J.J. Hall, D.J. Chaplin, M.L. Trawick, K.G. Pinney. Synthesis and biological evaluation of indole-based, anti-cancer agents inspired by the vascular disrupting agent 2-(3'-hydroxy-4'-methoxyphenyl)-3-(3'',4'',5''-trimethoxybenzoyl)-6-methoxy indole (OXi8006). *Bioorg Med Chem.* 21 (2013) 6831–6843.
- [18] P.C. Diao, Q. Li, M.J. Hu, Y.F. Ma, W.W. You, K.H. Hong, P.L. Zhao. Synthesis and biological

evaluation of novel indole-pyrimidine hybrids bearing morpholine and thiomorpholine moieties.

- 520 Eur J Med Chem. 134 (2017) 110–118.
- [19] P.L. Zhao, W.F. Ma, A.N. Duan, M. Zou, Y.C. Yan, W.W. You, S.G. Wu, One-pot synthesis of novel isoindoline-1,3-dione derivatives bearing 1,2,4-triazole moiety and their preliminary biological evaluation. Eur J Med Chem. 54 (2012) 813–822.
- [20] W.F. Ma, H.K. Yang, M.J. Hu, Q. Li, T.Z. Ma, Z.Z. Zhou, R.Y. Liu, W.W. You, P.L. Zhao, 525 One-pot synthesis and antiproliferative activity of novel 2,4-diaminopyrimidine derivatives bearing piperidine and piperazine moieties. Eur J Med Chem. 84 (2014) 127–134.
- [21] B. Zhang, Y.H. Li, Y. Liu, Y.R. Chen, E.S. Pan, W.W. You, P.L. Zhao. Design, synthesis and biological evaluation of novel 1,2,4-triazolo [3,4-b][1,3,4] thiadiazines bearing furan and thiophene nucleus. Eur J Med Chem. 103 (2015) 335–342.
- 530 [22] Q. Li, H.K. Yang, Q. Sun, W.W. You, P.L. Zhao. Design, synthesis and antiproliferative activity of novel substituted 2-amino-7,8-dihydropteridin-6(5H)-one derivatives. Bioorg Med Chem Lett. 27 (2017) 3954–3958.
- [23] M.J. Hu, B. Zhang, H.K. Yang, Y. Liu, Y.R. Chen, T.Z. Ma, L. Lu, W.W. You, P.L. Zhao, Design, synthesis and molecular docking studies of novel indole-pyrimidine hybrids as tubulin polymerization inhibitors. Chem Biol Drug Des. 86 (2015) 1491–1500.
- 535 [24] W.L. DeLano, DeLano Scientific, San Carlos, CA, USA, <http://www.pymol.org>, 2002.
- [25] Y.H. Li, B. Zhang, H.K. Yang, Q. Li, P.C. Diao, W.W. You, P.L. Zhao. Design, synthesis, and biological evaluation of novel alkylsulfanyl-1,2,4-triazoles as cis-restricted combretastatin A-4 analogues. Eur J Med Chem. 125 (2017) 1098–1106.
- 540 [26] Sybyl 7.3, Tripos Inc., 1699 South Hanley Road, St. Louis, MO 63144, U.S.A.
- [27] R.B.G. Ravelli, B. Gigant, P.A. Curmi, I. Jourdain, S. Lachkar, A. Sobel, M. Knossow. Insight into tubulin regulation from a complex with colchicine and a stathmin-like domain. Nature 428 (2004) 198–202.

545

550

555

Figure captions

560 **Fig. 1.** The structures of CA-4, representative 3-substituted indole derivatives with potent anti-tubulin activity
and the general structure of target compounds 6-34.

565 **Fig. 2.** Effect of compound **27** and CA-4 on cell cycle and apoptosis in BT549 cells. Flow cytometry analysis of
BT549 cells treated with **27** for 24 h. (A) Control; (B) **27**, 2 μM ; (C) **27**, 4 μM ; (D) **27**, 8 μM ; (E) CA-4, 8 μM .

Fig. 3. Effect of compound **27** on tubulin expression in BT549 cell. Cells were seeded on glass coverslips,
incubated with compound **27** (10 μM , 20 μM) for 6 h, then fixed and processed for confocal microscopy.

570

Fig. 4. Docked pose of **27** (cyan stick) overlayed with CA-4 (magenta) in colchicine binding site of tubulin. The
main interacting residues are shown and labeled. The black dashed lines are the potential H-bond between Cys241
(2.0 \AA), Thr179 (2.9 \AA), Asn258 (2.2 \AA). Final figure for docking pose was generated by PyMOL [24].

575

580

585

590

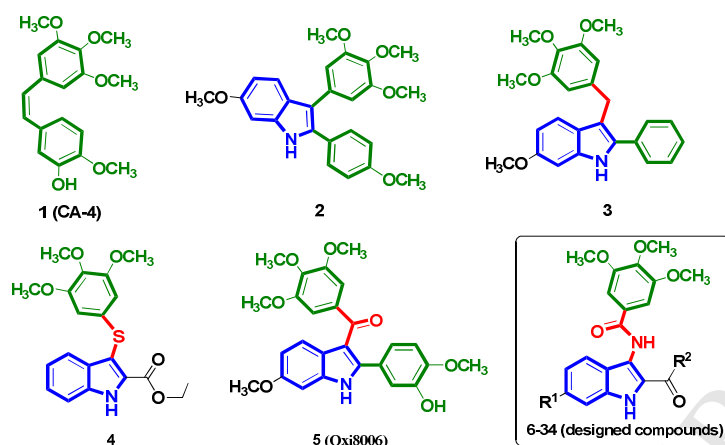


Fig. 1. The structures of CA-4, representative 3-substituted indole derivatives with potent anti-tubulin activity and the general structure of target compounds 6-34.

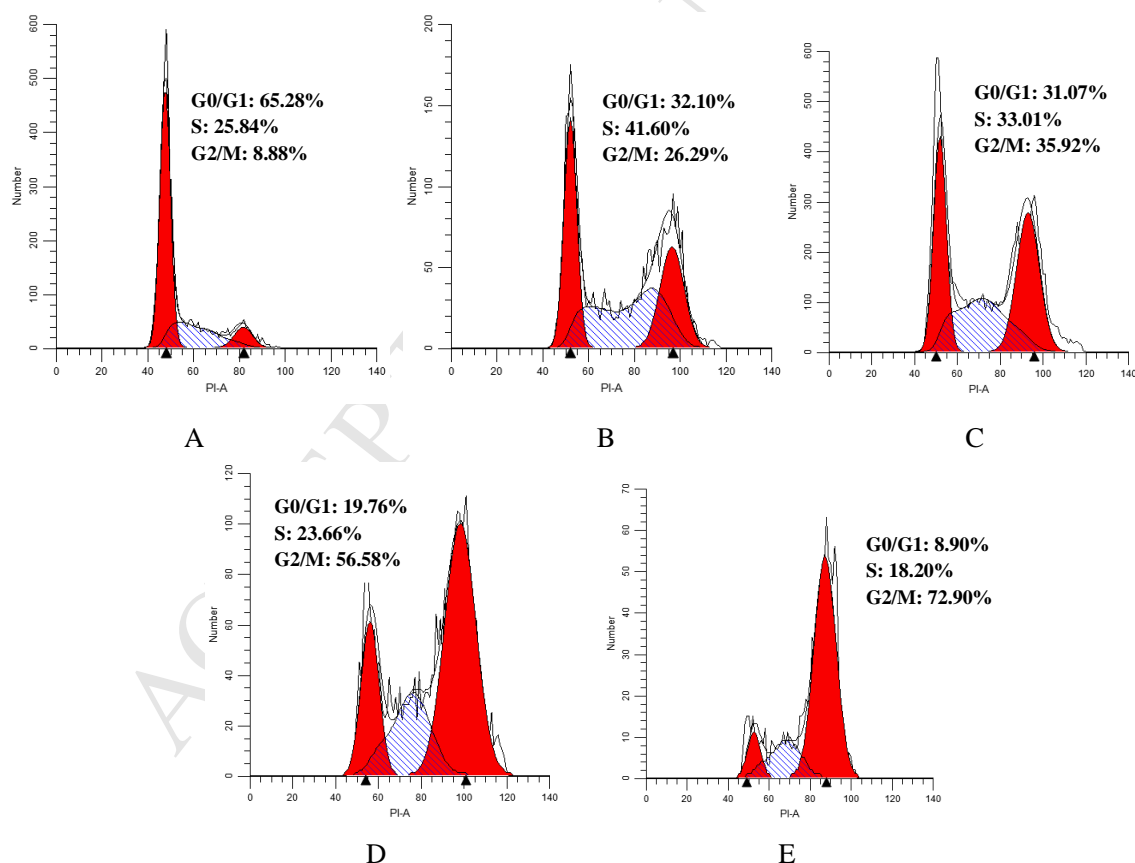


Fig. 2. Effect of compound **27** and CA-4 on cell cycle and apoptosis in BT549 cells. Flow cytometry analysis of BT549 cells treated with **27** for 24 h. (A) Control; (B) **27**, 2 μ M; (C) **27**, 4 μ M; (D) **27**, 8 μ M; (E) CA-4, 8 μ M.

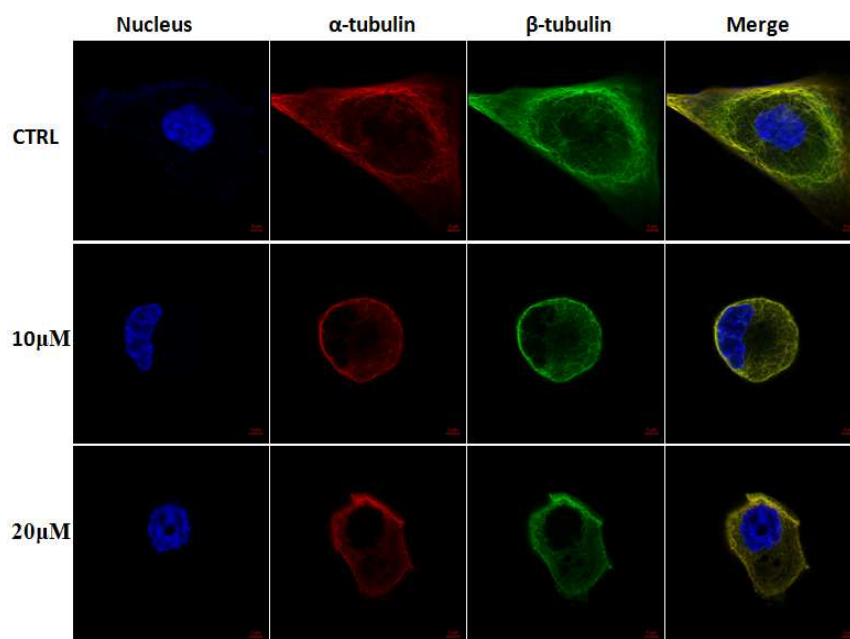


Fig.3. Effect of compound **27** on tubulin expression in BT549 cell. Cells were seeded on glass coverslips, incubated with compound **27** (10 μ M, 20 μ M) for 6 h, then fixed and processed for confocal microscopy.

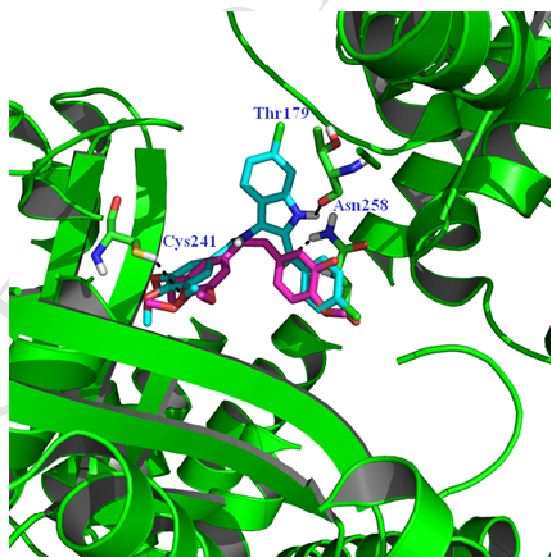
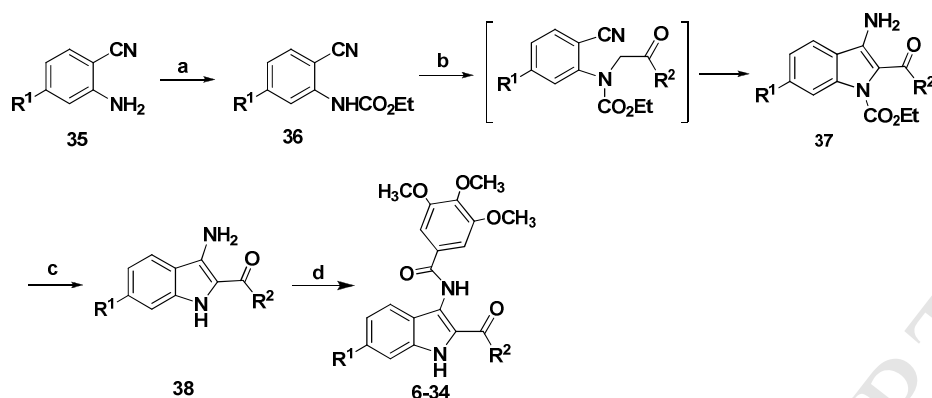


Fig. 4. Docked pose of **27** (cyan stick) overlaid with CA-4 (magenta) in colchicine binding site of tubulin. The main interacting residues are shown and labeled. The black dashed lines are the potential H-bond between Cys241 (2.8 Å), Thr179 (2.2 Å), Asn258 (2.7 Å). Final figure for docking pose was generated by PyMOL [24].



Scheme 1. Synthesis of the target compounds 6–34. Reagents and conditions: (a) ClCO_2Et , reflux; (b) K_2CO_3 , α -bromoketones, DMF, r.t.; (c) 2M NaOH, reflux; (d) 3,4,5-trimethoxybenzoyl chloride, Et_3N , THF, r.t.

620

625

Table 1 Cytotoxic activities of compounds 6–34 against a panel of human cancer cell lines

Comp.	R^1	R^2	<i>In vitro</i> cytotoxicity IC_{50} (μM) ^a					
			MCF-7	MDA-MB-231	BT549	T47D	MDA-MB-468	HS578T
6	CH_3	4- FC_6H_4	8.89±0.64	5.17±0.49	8.66±0.27	5.72±0.66	6.16±0.24	8.95±0.43
7	CH_3	4- $\text{CH}_3\text{C}_6\text{H}_4$	69.48±7.52	33.43±2.71	69.75±2.09	40.16±1.07	75.10±2.20	43.68±4.05
8	CH_3	C_6H_5	32.74±7.03	16.60±3.33	42.26±2.25	>100	>100	49.06±3.19
9	CH_3	4- ClC_6H_4	3.85±0.87	3.22±0.43	4.81±0.57	6.25±0.25	4.12±0.39	3.59±0.07
10	CH_3		>100	18.21±2.23	>100	>100	>100	>100
11	CH_3		>100	>100	>100	>100	>100	>100
12	CH_3		>100	>100	39.75±3.36	>100	>100	53.32±6.62
13	H	4- FC_6H_4	77.92±10.01	50.76±3.86	42.58±2.97	60.86±3.32	>100	>100
14	H	4- $\text{CH}_3\text{C}_6\text{H}_4$	50.00±14.35	12.61±1.78	17.07±0.87	20.06±2.04	14.52±0.99	50.49±2.26
15	H	C_6H_5	>100	17.22±2.04	>100	>100	>100	>100
16	H	4- BrC_6H_4	7.14±1.15	6.47±0.95	10.31±1.42	9.55±0.31	7.87±0.55	7.52±0.61
17	H		>100	>100	>100	>100	>100	22.24±1.42
18	H	3- $\text{CH}_3\text{OC}_6\text{H}_4$	>100	>100	65.53±7.13	53.39±3.25	>100	9.06±4.22
19	H		>100	>100	>100	>100	>100	29.57±1.13
20	H	4- $\text{CH}_3\text{OC}_6\text{H}_4$	10.70±0.77	34.96±2.92	10.37±0.23	5.56±0.37	7.09±0.78	>100
21	Cl	4- FC_6H_4	61.08±17.61	46.65±7.47	35.54±3.13	76.17±2.93	>100	>100
22	Cl	4- $\text{CH}_3\text{C}_6\text{H}_4$	34.33±2.98	33.65±0.61	25.05±2.09	16.65±0.34	5.79±0.09	14.19±0.54
23	Cl	C_6H_5	51.78±5.84	32.66±5.27	26.89±1.78	45.51±2.69	11.04±0.19	>100
24	Cl	4- $\text{CH}_3\text{OC}_6\text{H}_4$	17.62±0.40	9.17±1.01	11.14±0.43	11.09±1.31	8.61±0.51	15.93±1.27
25	Cl	3- $\text{CH}_3\text{OC}_6\text{H}_4$	>100	>100	>100	52.41±1.06	>100	>100
26	Cl	3- BrC_6H_4	23.02±2.47	26.75±1.12	8.42±1.06	14.07±0.61	20.79±0.34	4.10±0.27
27	Cl	4- ClC_6H_4	10.87±0.87	6.43±1.12	3.17±0.46	0.04±0.06	7.92±1.36	>100
28	Cl		>100	>100	>100	>100	>100	>100
29	Cl		47.46±3.29	>100	37.51±7.14	31.45±1.87	15.33±3.11	49.23±4.61
30	Cl	3,4- $\text{F}_2\text{C}_6\text{H}_4$	10.14±1.16	>100	51.25±5.85	>100	>100	64.57±5.73
31	Cl	3-OH-4- $\text{CH}_3\text{OC}_6\text{H}_4$	32.60±0.68	22.18±1.38	7.48±0.19	9.28±0.13	23.21±2.08	4.35±0.14

32	CH ₃ O	4-CH ₃ OC ₆ H ₄	79.27±3.05	48.84±2.76	18.20±0.13	6.30±0.52	26.38±1.36	10.44±0.66
33	CH ₃ O	C ₆ H ₅	>100	>100	>100	>100	>100	>100
34	CH ₃ O	4-CH ₃ C ₆ H ₄	>100	>100	>100	>100	>100	>100
CA-4 (nM)			3.00±0.65	3.17±0.57	1.71±0.44	1.89±0.34	1.55±0.18	1.36±0.23

^a 50% inhibitory concentration and mean ± SD of three independent experiments performed in duplicate.

630

Table 2 Tubulin polymerization inhibitory activities of representative selected compounds

Comp.	R ¹	R ²	Tubulin polymerization	
			% inhibition ^a	IC ₅₀ (μM)
6	CH ₃	4-FC ₆ H ₄	17	- ^b
9	CH ₃	4-ClC ₆ H ₄	15	-
16	H	3-BrC ₆ H ₄	37	-
20	H	4-MeOC ₆ H ₄	20	-
22	Cl	4-CH ₃ C ₆ H ₄	36	-
23	Cl	C ₆ H ₅	41	-
24	Cl	4-CH ₃ OC ₆ H ₄	47	-
26	Cl	3-BrC ₆ H ₄	25	-
27	Cl	4-ClC ₆ H ₄	59	9.5
31	Cl	3-OH-4-CH ₃ OC ₆ H ₄	30	-
32	CH ₃ O	4-MeOC ₆ H	25	-
CA-4			80	4.22

^a Compounds were tested at a final concentration of 10μM. ^b -: not tested.

635

Highlights

► Based on our previous work, a series of novel 3-amidoindole derivatives were synthesized. ► IC_{50} of compound **27** were 0.04, 3.17, and 6.43 μ M against T47D, BT549, and MDA-MB-231, respectively. ► Compound **27** exhibited remarkable anti-tubulin activity with IC_{50} of 9.5 μ M, compared to CA-4.